PAPER

Economically attractive route for the preparation of high quality magnetic nanoparticles by the thermal decomposition of iron(III) acetylacetonate

To cite this article: Fernando B Effenberger *et al* 2017 *Nanotechnology* **28** 115603

IOP Publishing Nanotechnology
Nanotechnology **28** (2017) 115603 (8pp) https://doi.org/10.1088/1361-6528/aa5ab0

Economically attractive route for the preparation of high quality magnetic nanoparticles by the thermal decomposition of iron(III) acetylacetonate

Fernando B Effenberger[1,4], Ricardo A Couto[1], Pedro K Kiyohara[2], Giovanna Machado[3], Sueli H Masunaga[2], Renato F Jardim[2] and Liane M Rossi[1]

[1] Departamento de Química Fundamental, Instituto de Química, Universidade de São Paulo, 05508-000 são Paulo, SP, Brazil
[2] Instituto de Física, Universidade de São Paulo, CP 66318, 05315-970, São Paulo, SP, Brazil
Q1 [3] Centro de Tecnologias Estratégicas do Nordeste (CETENE), Recife, PE, Brazil

E-mail: lrossi@iq.usp.br

Received 14 November 2016, revised 3 January 2017
Accepted for publication 13 January 2017
Published 13 February 2017

Abstract

The thermal decomposition (TD) methods are among the most successful in obtaining magnetic nanoparticles with a high degree of control of size and narrow particle size distribution. Here we investigated the TD of iron(III) acetylacetonate in the presence of oleic acid, oleylamine, and a series of alcohols in order to disclose their role and also investigate economically attractive alternatives for the synthesis of iron oxide nanoparticles without compromising their size and shape control. We have found that some affordable and reasonably less priced alcohols, such as 1,2-octanediol and cyclohexanol, may replace the commonly used and expensive 1,2-hexadecanediol, providing an economically attractive route for the synthesis of high quality magnetic nanoparticles. The relative cost for the preparation of Fe_3O_4 NPs is reduced to only 21% and 9% of the original cost when using 1,2-octanediol and cyclohexanol, respectively.

Supplementary material for this article is available online

Keywords: Brazilian MRS, magnetite, thermal decomposition, iron(III) acetylacetonate, oleic acid, oleylamine, 1,2-alkanediol

(Some figures may appear in colour only in the online journal)

1. Introduction

Magnetic nanoparticles (MNPs) have been attracting interest because of their unique magnetic properties and interesting technological and biomedical applications [1]. The magnetic properties are size-dependent and also strongly dependent on their degree of structural order, surface disorder, and interactions between the nanoparticles. Among various techniques developed for the synthesis of MNPs [2–6], the thermal decomposition (TD) methods have been the most successful in obtaining MNPs with high degree of crystallinity, size-control, and narrow particle size distribution [1, 2, 6–10]. However, mostly of the TD protocols made use of a complex mixture of reagents, which makes the synthesis expensive. TD methods allow the synthesis of various types of MNPs, such as magnetite [11], cobalt and nickel ferrites [2, 8, 10, 12], bimetallic [13, 14] as well as core–shell structures [15]. They are commonly performed with transition metal acetylacetonates and metal carbonyls [16]. However,

[4] Present address: Departamento de Engenharia Química, Centro Universitário da FEI, 09850-901 São Bernardo do Campo, SP, Brazil.

other precursors such as acetates [17], heterometallic complexes [18], and metal oleates [19] produced in a previous step from metal nitrates or chlorides [20–22] have also been reported [22, 23]. The TD methods are carried out in solvents with high boiling points, particularly dioctyl ether [2], which have boiling points close to 300 °C, respectively; allowing the reaction to occur at high reflux temperature, a feature responsible for the improvement of the degree of crystal order of the NPs. The TD of iron(III) acetylacetonate was also reported to occur at temperature as low as 170 °C in dibenzyl ether and oleylamine [24]. Non-conventional solvents, such as ionic liquids, for instance, allow the synthesis in different temperature ranges [25–27].

The synthesis of MNPs by TD of iron(III) acetylacetonate, first reported by Sun and co-authors [11, 28], suffered modifications over the years, but still preserves the reduction and/or decomposition of the metal complexes with the use of high boiling point ethers in the presence of oleic acid (OA), oleylamine (OAm), and an 1,2-alkanediol. Despite the large number of studies involving MNPs obtained by TD methods, the role of each reagent used in the synthesis is not fully understood, possibly due to multiple roles and various possible interactions between the metal precursor and each of the reagents, and also the interaction between reagents [24, 27, 29, 30]. Possible interactions discussed in the literature include the formation of an acid–base-complex between OA and OAm [31] and the coordination of OA with iron(III) to give iron(III) oleates [32], which was identified as an important synthesis intermediate. It has also been reported that MNPs may be obtained using OA as the only surfactant [33] or using barely OAm as surfactant [24], further indicating that MNPs can be obtained from different precursors and stabilized by different molecules. However, the preparation of magnetite NPs (Fe_3O_4) requires the reduction of 1/3 of the iron(III) ions present in solution into iron(II) ions. Such a reduction process has been attributed to either the 1,2-alkanediol [34] or OAm [24], which makes a controversial issue for establishing which one is the reducing agent.

Due to the high quality of the materials obtained by the TD methods, they are regarded as one of the most promising route for obtaining MNPs. In the TD synthesis, originally reported by Sun and co-authors [28], the long-chain dialcohol 1,2-hexadecanediol was used for the decomposition of $Fe(acac)_3$ in the presence of OA and OAm, resulting in high quality Fe_3O_4 NPs with mean diameter close to 4 nm, spherical shape, and narrow particle size distribution. This dialcohol corresponds to about 90% of the cost of the chemicals used in the reaction, being a problem for product development, scale-up, and commercialization, hence it would be of interest to substitute it without compromising the high quality of the material. Within this context, we have suggested previously that 1,2-hexadecanediol may be substituted, for example, by 1,2-octanediol without compromising the high quality of Fe_3O_4 NPs [35]. Continuing our efforts on this subject, we describe here our investigations on the TD of $Fe(acac)_3$ using much less expensive reagents to produce MNPs with controlled size and morphology, and economically more attractive. The relative cost of each chemical and of each preparation discussed in this work is given in table S1. As an example, the preparation of Fe_3O_4 NPs using 1,2-octanediol corresponds to 21% of the cost for the preparation of Fe_3O_4 NPs using 1,2-hexadecanediol.

2. Results and discussion

The TD method for the synthesis of MNPs, introduced by Sun and co-authors [11, 28], is typically based on the decomposition of iron(III) acetylacetonate in a high boiling point ether and in the presence of OA, OAm, and an 1,2-alkanediol. We first evaluate the TD synthesis of Fe_3O_4 NPs using similar amounts of metal precursor and solvent, but varying the nature of the other components of the synthesis. Iron (III) acetylacetonate (2 mmol) was then used as the metal precursor and diphenylether (DPE) as a solvent (20 ml). The TD reaction was performed in the presence of the following reagents: OA alone (6 mmol), OAm alone (4 mmol), and a mixture of OA (6 mmol) and OAm (4 mmol). The results were compared with those from our previously reported synthesis [35], which was performed in the presence of OA (6 mmol), OAm (4 mmol), and 1,2-octanediol (10 mmol). The mixture remained under stirring in nitrogen atmosphere and refluxed for 2 h. After purification, all MNPs could be dispersed in toluene or obtained as a powder after vacuum drying.

The morphology, average size and size distribution of the Fe_3O_4 NPs were analyzed by transmission electron microscopy (TEM). The micrographs are displayed in figures 1(a)–(d) and the size distribution histograms, which were fitted with a lognormal distribution, are presented in the supplementary material (figure S1). The TD reaction performed in the presence of OAm, as the only one stabilizing agent, resulted in a material with a poor morphology and size control as shown in figure 1(a). This behavior suggests a poor interaction of the amine groups with the iron oxide surfaces and, consequently, a highly agglomerated material. The TD reaction performed in the presence of OA, as the only one stabilizing agent, resulted in a material, as displayed in figure 1(b), with better dispersion than the one synthesized in OAm. However, the latter still exhibits a very poor size control of the NPs. The micrograph of figure 1(b) confirms such a statement and displays nearly spherical nanoparticles but with a bimodal size distribution with mean diameters of 3.3 nm ($\sigma = 0.39$) and 9.0 nm ($\sigma = 0.13$). Ostwald ripening, caused by a large excess of free OA, seems to be a reasonable explanation for the occurrence of the bimodal size distribution of the Fe_3O_4 NPs. Moreover, the strong interaction between OA and the iron oxide surface is able to maintain the MNPs separated from each other and very stable in toluene solution. As far as this point is concerned, in situ IR spectroscopy experiments have provided evidence for the adsorption of OA to the magnetite surface as a carboxylate [31], lending credence to our analysis.

The TD synthesis performed with a mixture of OA and OAm (without 1,2-alkanediol) resulted in a material with quite a uniform size distribution of MNPs, as shown in the

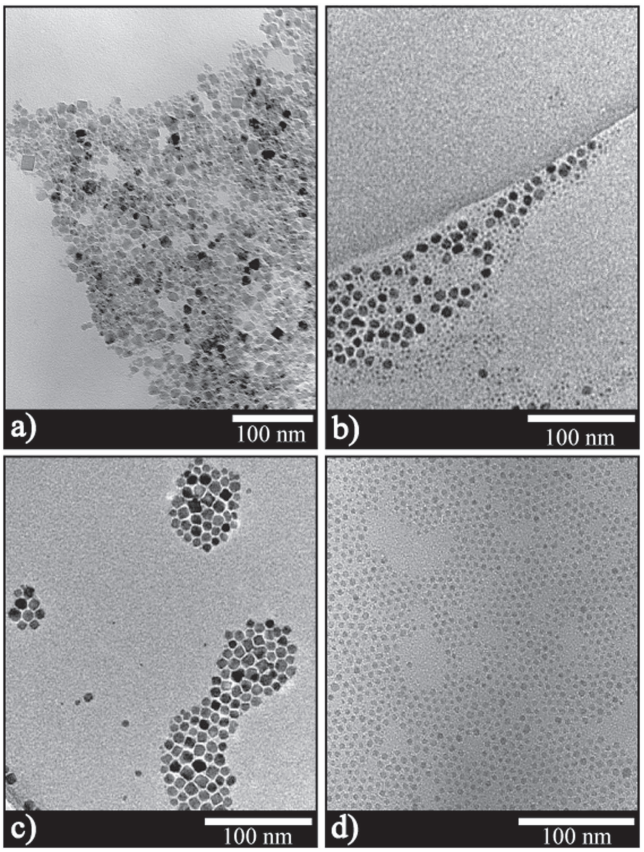

Figure 1. TEM micrographs of magnetite Fe_3O_4 NPs obtained by thermal decomposition of $Fe(acac)_3$ in DPE and with the following additives: (a) OAm; (b) OA; (c) a mixture of OAm and OA; and (d) a mixture of OAm, OA, and 1,2-octanediol.

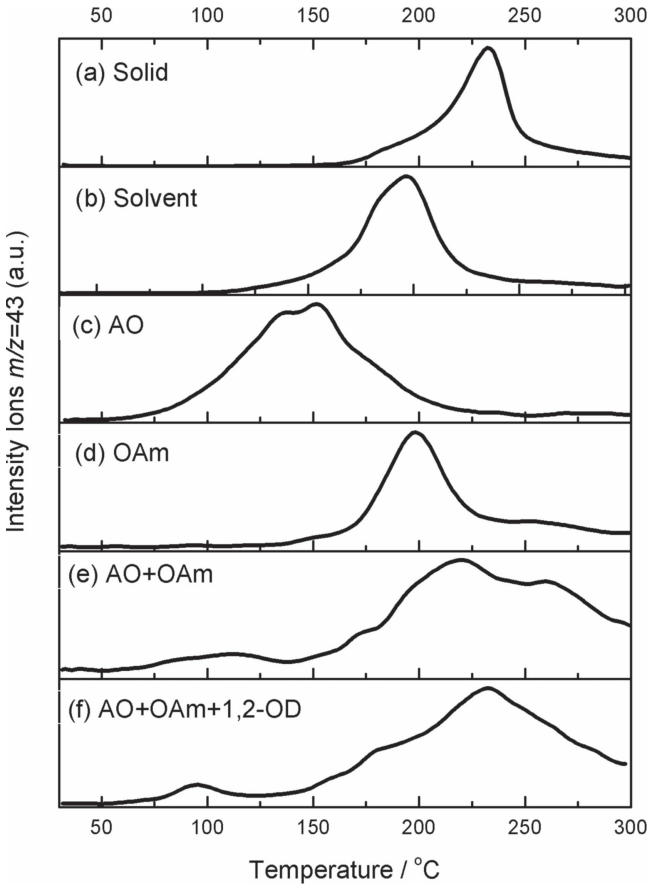

Figure 2. Mass analysis data of the gas evolved during the thermal analysis (measured by TG-MS) of solutions containing $Fe(acac)_3$: (a) solid; (b) in DPE; (c) in DPE and OA; (d) in DPE and OAm; (e) in DPE, OA and OAm; and (f) in DPE, OA, OAm and 1,2-octanediol.

micrograph of figure 1(c), which displays faceted nanoparticles with a mean diameter of 9.0 nm ($\sigma = 0.17$). The amount of additives has not been changed in the synthesis, a parameter that could be used for tuning the size and morphology of the MNPs [36]. In fact, we have observed that by increasing the amount of stabilizer results in an increase of the stability of the organic phase, further reducing centrifugation efficiency and yield of isolated nanoparticles.

For comparison, we have also performed the TD synthesis in the presence of OA, OAm, and 1,2-octanediol, as reported elsewhere [35], which resulted in reproducible samples with well-dispersed spherical shaped nanoparticles of 5.5 nm with narrow size distribution ($\sigma = 0.12$) (figure 1(d)). It is interesting to notice that the absence of the 1,2-alkanediol in the TD synthesis, performed under similar conditions, resulted in the growth of faceted NPs with mean diameter of ~9 nm. This behavior suggests a strong influence of the 1,2-alkanediol on the TD process, contributing to the improvement of the NPs dispersion, size control, and size distribution. It is somewhat difficult to determine precisely how this molecule is affecting the nucleation or crystal growth process, but studies are underway in order to clarify this point.

Thermogravimetry coupled to mass spectrometry (TG-MS) was then used to evaluate the temperature of decomposition of iron(III) acetylacetonate using similar conditions as in the TD synthesis. The ion current of each m/z value measured in the gas evolved during the thermal analysis is proportional to the evolution rate of the corresponding fragment. Figure 2 shows the ion intensity of $m/z = 43$ (CH_3CO^+) as a function of temperature, which can be used to accompany the decomposition of acetylacetonate ions that are either free or weakly bound to Fe^{3+} ions. These curves indicate the temperature range for the decomposition of the acetylacetonate-iron complex, but may not correspond to the temperature of formation of the MNPs. Kwon *et al* [23] reported kinetic studies of the formation of iron oxide nanocrystals obtained from the TD of iron-oleate complex by TG-MS and *in situ* magnetic measurements. Their results suggest that the iron-oleate complex is decomposed into intermediate species that act as the minimum building units of iron oxide nanocrystals. The iron oxide nanocrystals are then formed at temperatures above 310 °C during the heating procedure.

The TG-MS results show that the temperature of decomposition of $Fe(acac)_3$ is affected by the different compounds used in the TD synthesis. The iron(III) acetylacetonate complex in solid state decomposes at $T > 200$ °C (T_{max} 232 °C) (figure 2(a)). In the presence of solvent (DPE), the decomposition temperature was found to decrease about 30 °C (T_{max} 200 °C) (figure 2(b)). It is worth noting that the solvent and all components used in the synthesis were tested separately and they did not show any signal at $m/z = 43$ in

the temperature range studied (figure S4). In the presence of OA and DPE, the decomposition temperature decreased further, almost 200 °C, reaching the lower decomposition temperature observed (broad range from 70 °C to T_{max} 137 °C) (figure 2(c)). In the presence of OAm and DPE, the decomposition profile of the iron (III) acetylacetonate complex is rather similar to the reaction in solvent alone (figure 2(d)). In the presence of OA, OAm, and DPE, the decomposition temperature increased to $T > 200$ °C (T_{max} 220 °C) with signs of decomposition in a broad temperature range from 70 °C to 300 °C (figure 2(e)). The addition of 1,2-octanediol to the mixture of OA, OAm, and DPE caused no appreciable changes in the decomposition profile obtained with mixtures of OA and OAm (figure 2(f)). These results suggest that OAm, which has little effect on the temperature of decomposition of $Fe(acac)_3$ (figure 2(d)), does not coordinate to the Fe^{3+} ions and, therefore, does not participate in a ligand exchange reaction with the acetylacetonate. The lack of size control of the NPs prepared in OAm only also suggests that OAm does not adsorb to the MNPs surfaces. On the other hand, the OA causes the largest decrease in the temperature of decomposition of $Fe(acac)_3$ (figure 2(c)). Such a difference may be attributed to a ligand exchange reaction occurring at lower temperature leading to the formation of iron(III)-oleate, which is the true precursor for the MNPs. Oleic acid also adsorbs strongly to the MNPs surfaces and the occurrence of bimodal size distributions, as discussed above, strongly suggests an ongoing Ostwald ripening process. The combination of OA and OAm resulted in an increase in the decomposition temperature to $T > 200$ °C, and it seems to prevent the formation of iron(III)-oleate, which decomposes at lower temperature.

The effect of including OAm in the TD synthesis can be attributed to the formation of an acid–base complex of OA and OAm $RCOO^-$:RNH_3^+, as suggested by Klokkenburg *et al* [31] and supported by molecular mechanics modeling studies by Harris *et al* [37]. Moreover, an AO molecule cannot interact at the same time with OAm and with the magnetite surface, which allowed the nanoparticles to grow bigger than with either surfactant alone. The addition of 1,2-octanediol to the mixture of OA and OAm does not affect the temperature of decomposition of $Fe(acac)_3$, which suggests that it does not interfere in the acid–base complex of OA and OAm and, as expected, it does not participate in a ligand exchange reaction with the acetylacetonate. However, the presence of 1,2-octanodiol is responsible for a decrease in the size of the MNPs and narrowing of the particle size distribution. The decrease on the particle size suggests at least a secondary interaction of 1,2-octanodiol with the iron oxide surface through the surfactant layers (OA is still the one expected to coordinate to the iron oxide surfaces). A practical implication of our findings is that the presence of 1,2-octanediol provided the best condition for the synthesis of MNPs, even though our understanding of the formation mechanism of these uniform-sized nanocrystals is still very limited.

We thus studied the substitution of the 1,2-alkanediol by a series of other alcohols. The reactions were carried out while maintaining the standard mixture of metal precursor (2 mmol), OA (6 mmol), OAm (4 mmol), and DPE (20 ml). The replacement of the dialcohol (10 mmol) was made by adding 10 mmol of each of the following reagents: 1,2-hexanediol, 1,6-hexanediol, 1-hexanol, cyclohexanol, 2-ethylhexanol and 1-octadecanol. The mixture remained under stirring in nitrogen atmosphere and refluxed for 2 h. After purification, all MNPs could be dispersed in toluene or obtained as a powder after vacuum drying. The morphology, average size and size distribution of the nanoparticles produced in different conditions were analyzed by TEM. The micrographs are displayed in figures 3 and 4. The size distribution histograms, which were fitted by using a lognormal function, are found in the supplementary material (figures S2 and S3).

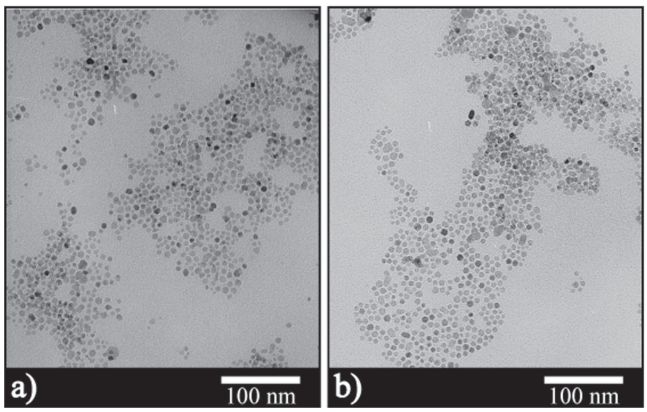

Figure 3. TEM micrographs of magnetite nanoparticles obtained by thermal decomposition of $Fe(acac)_3$ in DPE, OA, OAm and with the following alcohols: (a) 1,6-hexanediol, and (b) 1,2-hexanediol.

The results shown in figure 3 indicate that, when the chain length of the 1,2-alkanediol is decreased to six carbons, nearly spherical MNPs of 5.7 nm with a narrow particle size distribution ($\sigma = 0.19$) are still obtained, as displayed in figure 3(b). Comparing the series of 1,2-alkanediol with C16 [28], C8 (figure 1(d)), and C6 (figure 3(b)), only small changes in the MNPs morphology and size are noticed. Terminal OH-groups of 1,6-hexanediol were found to be less efficient in controlling the growth of the NPs when compared to the 1,2-hexanediol. The size of the MNPs increased to 6.3 nm and the size distribution was broadened ($\sigma = 0.27$), as shown in figure 3(a). These results suggest that the ligand with –OH groups in 1,2-position in the alkyl chain may be responsible for a better size control than –OH groups in 1,6-position. In order to further investigate the influence of the alcohol in the particle growth mechanism, we compared the TD synthesis in the presence of linear (1-hexanol) and sterically hindered monoalcohols such as cycloexanol and 2-ethylhexanol. 1-Hexanol provided a poorer size-control, resulting in a polydisperse sample whose morphology is shown in figure 4(a). On the other hand, cyclohexanol (bulk chain) provided a better control on particle size of 5.2 nm ($\sigma = 0.23$), as seen in the micrograph of figure 4(b). The bulkier molecule of 2-ethylhexanol provided an excellent size control and reduction of the average size to a value comparable to that reported with 1,2-hexadecanediol. The sample

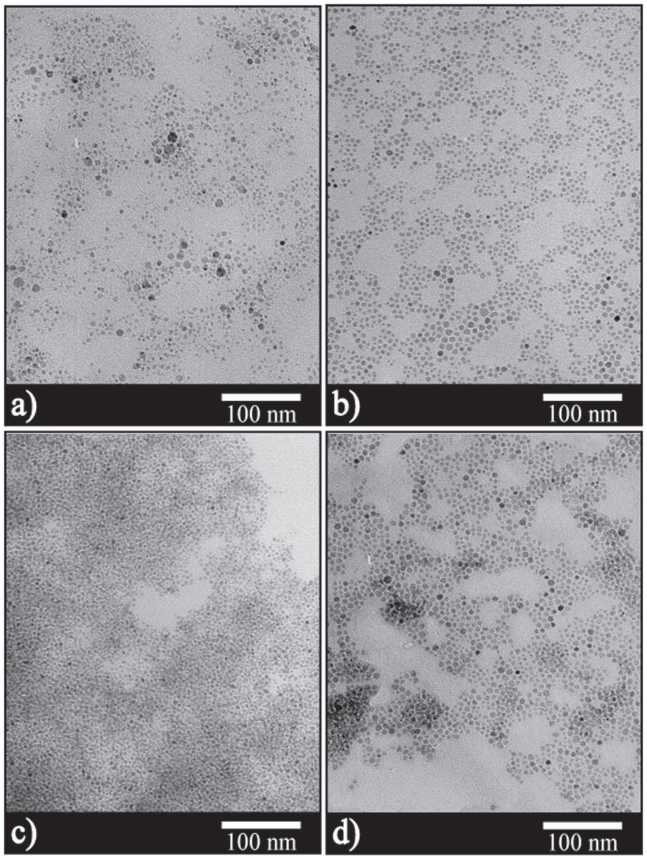

Figure 4. TEM micrographs of magnetite nanoparticles obtained by thermal decomposition of $Fe(acac)_3$ in DPE, OA, OAm and with the following alcohols: (a) hexanol, (b) cyclohexanol, (c) 2-ethylhexanol, and (d)1-octadecanol.

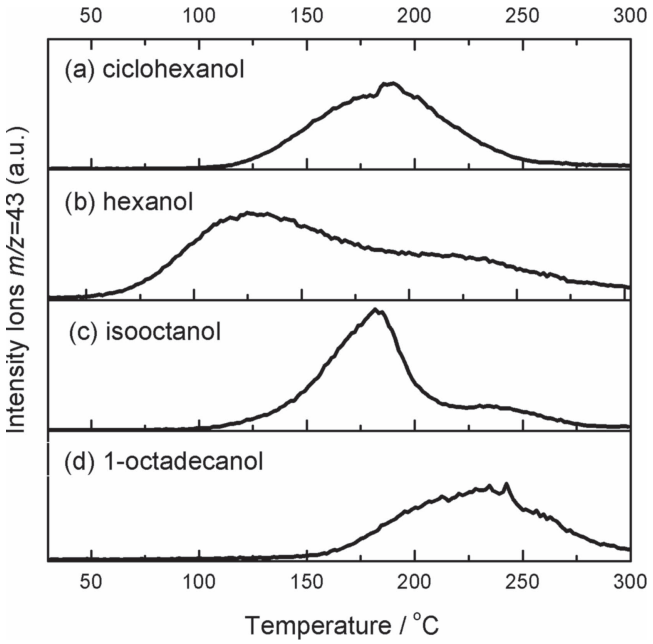

Figure 5. Mass analysis data of the gas evolved during the thermal analysis (measured by TG-MS) of solutions containing $Fe(acac)_3$, OA, OAm, DPE, and (a) cyclohexanol; (b) hexanol; (c) 2-ethylhexanol; and (d) 1-octadecanol.

prepared by decomposition of $Fe(acac)_3$ in the presence of AO, OAm and 2-ethylhexanol resulted in Fe_3O_4 nanoparticles with mean diameter of 4.1 nm ($\sigma = 0.21$), as displayed in figure 4(c). When the Fe_3O_4 nanoparticles prepared in the presence of a long chain alkane alcohol (1-octadecanol) is compared to a 1,2-alkanediol, it seems that the steric effect prevails. The sample prepared by decomposition of $Fe(acac)_3$ in the presence of AO, OAm and 1-octadecanol resulted in Fe_3O_4 nanoparticles with mean diameter of 5.6 nm ($\sigma = 0.19$), as shown in figure 4(d), which is similar to the average value obtained with 1,2-octanediol. The total cost for the preparation of Fe_3O_4 NPs using cyclohexanol corresponds to 9% of the cost for the preparation of Fe_3O_4 NPs using 1,2-hexadecanediol (attributed as 100% in table S1), which represents an economically attractive route.

In order to shed some light on the role of the alcohols during the TD of $Fe(acac)_3$ in the presence of OA and OAm, the TD reaction in the presence of the series of monoalcohols was studied by TG-MS (figure 5). All reactions were performed in a mixture of $Fe(acac)_3$, OA, OAm, and DPE, respecting the same proportion used in the synthesis of the Fe_3O_4 nanoparticles. In the presence of sterically hindered alcohols (cyclohexanol and 2-ethylhexanol), the decomposition profile of the iron(III) acetylacetonate complex is quite similar to the reaction in solvent alone (see figure 2(b)) and OAm alone (see figure 2(d)). The decomposition occurs in the temperature range from 100 °C to 250 °C (T_{max} 190 °C) (figures 5(a) and (c)). These results suggest that sterically hindered alcohols block the effect of OA in the decomposition of $Fe(acac)_3$, and the whole system behaves like it is running in OAm only. However, they provide better size control than in OAm alone, suggesting that they are acting as co-surfactant with some interaction with OA containing surfactant layers. In the presence of 1-hexanol, the decomposition temperature decreased to $T < 100$ °C (T_{max} 125 °C) with signs of decomposition in a broad temperature window ranging from 50 °C–300 °C (figure 5(b)). It is surprising that 1-hexanol causes a large decrease in the temperature of decomposition of $Fe(acac)_3$, displaying a behavior similar to OA alone (figure 2(c)). This result indicates that 1-hexanol provides a condition for the ligand exchange reaction between acetylacetonate and OA to occur, probably due to the breaking of the acid–base complex of OA and OAm. This alcohol does not provide good size control (figure 4(a)), which is also the case for OA alone (figure 1(b)). In the presence of 1-octadecanol, the decomposition temperature increased to $T > 200$ °C (T_{max} 230 °C) with decomposition occurring in the temperature range from 150 °C–300 °C (figure 5(d)). The long chain monoalcohol increases the decomposition temperature to $T > 200$ °C and display a decomposition profile similar to the reaction in OA and OAm (with or without 1,2-octanediol) (see figures 2(e), (f)). The size control and TG-MS results suggest that 1-octadecanol behaves similarly to 1,2-octanediol: it does not interfere in the acid–base complex of OA and OAm, nor does it participate in a ligand exchange reaction with the acetylacetonate.

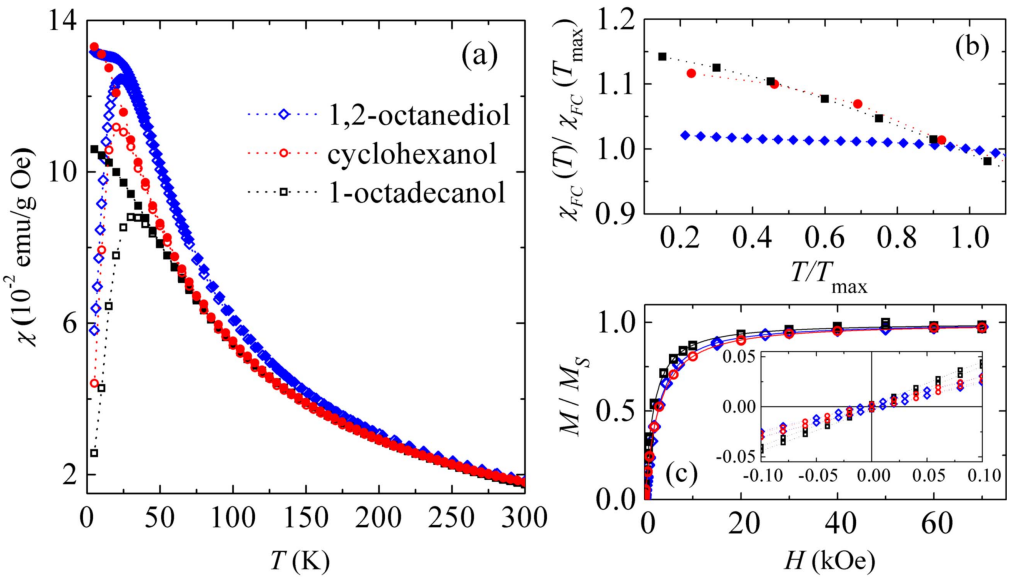

Figure 6. (a) Magnetic susceptibility as function of temperature, $\chi(T)$, measured under ZFC (open symbols) and FC (solid symbols) conditions of MNPs prepared by TD of $Fe(acac)_3$ in the presence of 1,2-octanediol (prism), cyclohexanol (circle), and 1-octadecanol (square) applying a magnetic field of $H = 50$ Oe. (b) Representation of the $\chi_{FC}(T)/\chi_{FC}(T_{max})$ versus T/T_{max} for the MNPs. The dotted lines are guides to the eyes. (c) Magnetization as a function of applied magnetic field, $M(H)$, measured at 300 K. The solid lines are fits using equation (1). The inset shows an expanded view of the data at low magnetic field.

Magnetic measurements were performed to further investigate the interaction between the MNPs synthesized in the presence of 1,2-octanediol ($d = 5.5$ nm), cyclohexanol ($d = 5.2$ nm), and 1-octadecanol ($d = 5.6$ nm). The magnetization M, or the magnetic susceptibility $\chi(T) = M(T)/H$, as a function of the applied magnetic field at 300 K, $M(H)$, and cycles of zero field cooled (ZFC) and field cooled (FC), measured under $H = 50$ Oe and in a large range of temperature, were performed to evaluate the magnetic properties of the NPs. Selected $M(H)$ and $\chi(T) = M(T)/H$ curves are shown in figure 6.

The $M(H)$ curves taken at 300 K showed no hysteresis for all samples, with negligible coercive field, and remnant magnetization. These results indicate that the MNPs are in the superparamagnetic state at room temperature. Furthermore, the values of saturation magnetization M_S at 300 K were 80, 64 and 44 emu g^{-1} for samples prepared in the presence of 1,2-octanediol, cyclohexanol and 1-octadecanol, respectively. These values correspond to over 50% of the bulk M_S of magnetite and are in agreement with the experimental ones obtained for other Fe_3O_4 NP systems found in the literature [6]. We have also obtained a rough estimate of the magnetic moment distribution of the assemblies of NPs from the fittings of the $M(H)$ data, by using the Langevin function [38]:

$$\frac{M(H)}{M_S} = \frac{\int_0^\infty \mu \mathrm{L}\left(\frac{\mu H}{k_B T}\right) f(\mu)\,\mathrm{d}\mu}{\int_0^\infty \mu f(\mu)\,\mathrm{d}\mu}, \qquad (1)$$

where M_S is the saturation magnetization, μ the magnetic moment, $f(\mu)$ the lognormal distribution of μ, and $L(\mu H/k_B T) = \coth(\mu H/k_B T) - 1/(\mu H/k_B T)$ the Langevin function. The width of magnetic distribution resulted in similar values of 0.71 and 0.73 for samples prepared in the presence of cyclohexanol and 1-octadecanol, respectively, corresponding to a width of size distributions of $\sigma = 0.24$ in both samples. This result is in agreement with the values extracted from TEM analysis, i.e., $\sigma = 0.23$ and 0.19 for samples prepared in the presence of cyclohexanol and 1-octadecanol, respectively. We also obtained similar values of the median magnetic moment, which correspond to a magnetic diameter of 4.0 and 4.6 nm for the samples prepared in the presence of cyclohexanol and 1-octadecanol, respectively. However, the $\chi_{ZFC}(T)$ curves for the sample prepared in 1-octadecanol exhibit a maximum at $T_{max} \sim 33$ K, which value is 1.5 times higher than 22 K obtained for the sample prepared in the presence of cyclohexanol. The dipolar interaction between MNPs was not taken into account in the analysis made above because this effect may be similar for both samples, which contain the same average 73 wt% of magnetic material. This procedure may lead to a slightly smaller apparent size if compared to TEM results [38]. Despite the fact that $\chi_{ZFC}(T)$ curves are more sensitive to dipolar interactions between particles [39], the difference observed in T_{max}, which is related to the blocking temperature (T_B) of the NPs, is certainly due to the small difference in the mean particle size. We obtained the ratio $T_B(\text{1-octadecanol})/T_B(\text{cyclohexanol}) = \langle V\rangle^{\text{1-octadecanol}}/\langle V\rangle^{\text{cyclohexanol}} = 1.5$ by taking the magnetic diameter and assuming the same value K and $\ln(\tau/\tau_0)$ for both samples in the equation $T_B = K\langle V\rangle/k_B \ln(\tau/\tau_0)$. Here, K is the anisotropy constant, k_B the Boltzmann's constant, τ the measuring time, and τ_0 the attempt time. Therefore, the higher T_{max} value for the Fe_3O_4 MNPs prepared in the presence of 1-octadecanol is primarily due to size effect. In fact, the effect of dipolar interaction in the magnetic properties for both samples is similar, as shown in the normalized $\chi_{FC}(T)$ curves in figure 6(b). The $\chi_{ZFC}(T)$

curve for the sample prepared in the presence of 1,2-octanediol exhibits a maximum at $T_{max} \sim 23$ K, which value is similar to the one obtained for the sample prepared in the presence of cyclohexanol and 2/3 of the ~33 K obtained for the sample prepared in the presence of 1-octadecanol. However, a significant narrower in the width of the magnetic distribution for the sample prepared in 1,2-octanediol of 0.54, corresponding to a width of size distribution of $\sigma = 0.18$, does not allow extracting information on the dipolar interactions by a comparison of those T_{max} values only. Nonetheless, the normalized $\chi_{FC}(T)$ curve of the sample prepared in 1,2-octanediol (figure 6(b)) exhibits a tendency to saturation in the whole range of temperature studied, a feature which is not observed in the other two samples. Such a tendency to saturation of $\chi_{FC}(T)$ indicates an increase of the dipolar interactions between nanoparticles in the sample prepared in 1,2-octanediol [39, 40]. As a matter of fact, the magnetic properties of all samples displayed here clearly indicate that they are suitable for many different biological and medical applications such as in diagnostic tests assays for early detection of diseases, noninvasive imaging, and drug development to be used as targeted drug delivery systems.

3. Experimental

3.1. Synthetic procedures

Magnetite nanoparticles were obtained according to the following procedure: 2 mmol of $Fe(Acac)_3$, 6 mmol of OA, 4 mmol of OAm, 10 mmol of alcohol (1,2-octanediol, 1,2-hexanediol, 1,6-hexanediol, 1-hexanol, cyclohexanol, 2-ethylhexanol and 1- octadecanol) and 20 ml of DPE were added to a three neck round bottom flask under inert atmosphere. A condenser was adapted and the mixture was refluxed (265 °C) under stirring for 2 h. A black precipitate was formed after the addition of ethanol (80 ml), which was removed from the reaction mixture by centrifugation (7000 rpm, 10 min). The MNPs were washed with ethanol (3 × 50 ml) and redispersed in toluene, leading to the formation of a stable colloidal solution.

For comparison, three samples were prepared similarly, in the absence of alcohol, using 2 mmol of $Fe(Acac)_3$, 20 ml of DPE and the corresponding amount of AO only, OAm only or the mixture of OA and OAm.

3.2. Materials and methods

TEM micrographs were obtained on a Philips CM 200 microscope operating at an accelerating voltage of 200 kV (IF-USP). Samples for TEM observations were prepared by placing a drop of a toluene solution containing the dispersed NPs in a carbon coated copper grid. The metal particle size distribution was estimated from the measurement of about 800–1000 particles, assuming spherical shape, found in an arbitrarily chosen area in enlarged micrographs. TD studies were performed by means of thermogravimetric/mass spectrometry (TG/MS) using a NETZSCH STA 409 PC LUXX connected to a NETZSCH Q MS 403 C—quadrupole mass spectrometer. Nitrogen purge gas was used with a flow rate of 50 ml min^{-1}. The samples were heated from 30 °C to 300 °C at a heating rate of 10 °C min^{-1}. Magnetization measurements $M(T, H)$ in applied magnetic fields between ±7 T and for temperatures ranging from 2 to 300 K, were performed in powders conditioned in gelatin capsules with a Quantum Design SQUID magnetometer. The magnetic susceptibility data, $\chi(T) = M(T)/H$, were obtained under both ZFC, $\chi_{ZFC}(T)$, and field-cooled (FC), $\chi_{FC}(T)$, conditions in a temperature range of 2–300 K under low (<500 Oe) applied magnetic fields.

4. Conclusions

The preparation of Fe_3O_4 NPs by the TD of $Fe(acac)_3$ in the presence of oleic acid, oleylamine, and an 1,2-alkylalcohol become very popular, but very little is known about the role of the most expensive reagent 1,2-alkanediol, which contribute to about 90% of the reagents cost. We conclude here that the presence of both OA and OAm is very important to achieve better size control on the TD synthesis, which has a close relation with the formation of a complex between OA and OAm that increases the temperature of decomposition of the metal precursor. The presence of mono- or di-alcohols, which did not affect the OA–OAm interaction or the decomposition temperature, improved the size control. They affected the crystal growth process, suggesting that they act as co-surfactants through secondary interaction with the iron oxide through the OA containing surfactant layers. The simple replacement of 1,2-hexadecanediol by 1,2-octanediol represents a reduction of the total cost to only 21% of the original cost for the preparation of high quality Fe_3O_4 NPs. Moreover, other long alkyl-chain or sterically hindered monoalcohols can be used in the TD reaction for the synthesis of Fe_3O_4 NPs without compromising their desirable morphology as well as size and shape. The expensive di-alcohol may be replaced by some affordable monoalcohols, such as cyclohexanol, further reducing the relative cost to only 9% of the original, resulting in an economically attractive route for the synthesis of high quality MNPs. From a practical viewpoint, the Fe_3O_4 NPs samples studied exhibited suitable magnetic properties for most applications of MNPs as the ones prepared with costly reagents.

Acknowledgments

This research was supported by Brazil's agencies Conselho Nacional de Desenvolvimento Científico e Tecnológico (CNPq), Coordenação de Aperfeiçoamento de Pessoal de Nível Superior (CAPES), and Fundação de Amparo à Pesquisa do Estado de São Paulo (FAPESP). The authors thank Professor Ana Maria Costa Ferreira (Instituto de Química, Universidade de São Paulo) for the TG-MS analysis (FAPESP Grant 05/60596-8).

References

[1] Lee J, Zhang S and Sun S 2013 High-temperature solution-phase syntheses of metal-oxide nanocrystals *Chem. Mater.* **25** 1293–304

[2] Hyeon T 2003 Chemical synthesis of magnetic nanoparticles *Chem. Commun.* **2003** 927–34

[3] Park J, Joo J, Kwon S G, Jang Y and Hyeon T 2007 Synthesis of monodisperse spherical nanocrystals *Angew. Chem. Int. Ed.* **46** 4630–60

[4] Gijs M A, Lacharme F and Lehmann U 2009 Microfluidic applications of magnetic particles for biological analysis and catalysis *Chem. Rev.* **110** 1518–63

[5] Laurent S *et al* 2008 Magnetic iron oxide nanoparticles: synthesis, stabilization, vectorization, physicochemical characterizations, and biological applications *Chem. Rev.* **108** 2064–110

[6] Frey N A, Peng S, Cheng K and Sun S 2009 Magnetic nanoparticles: synthesis, functionalization, and applications in bioimaging and magnetic energy storage *Chem. Soc. Rev.* **38** 2532–42

[7] Hyeon T, Lee S S, Park J, Chung Y and Na H B 2001 Synthesis of highly crystalline and monodisperse maghemite nanocrystallites without a size-selection process *J. Am. Chem. Soc.* **123** 12798–801

[8] Lu L T *et al* 2015 Synthesis of magnetic cobalt ferrite nanoparticles with controlled morphology, monodispersity and composition: the influence of solvent, surfactant, reductant and synthetic conditions *Nanoscale* **7** 19596–610

[9] Hufschmid R *et al* 2015 Synthesis of phase-pure and monodisperse iron oxide nanoparticles by thermal decomposition *Nanoscale* **7** 11142–54

[10] Eom Y, Abbas M, Noh H and Kim C 2016 Morphology-controlled synthesis of highly crystalline Fe_3O_4 and $CoFe_2O_4$ nanoparticles using a facile thermal decomposition method *RSC Adv.* **6** 15861–7

[11] Sun S H, Murray C B, Weller D, Folks L and Moser A 2000 Monodisperse FePt nanoparticles and ferromagnetic FePt nanocrystal superlattices *Science* **287** 1989–92

[12] Peng S, Xie J and Sun S 2008 Synthesis of Co/MFe_2O_4 (M = Fe, Mn) core/shell nanocomposite particles *J. Solid State Chem.* **181** 1560–4

[13] Mott D *et al* 2011 Bismuth, antimony and tellurium alloy nanoparticles with controllable shape and composition for efficient thermoelectric devices *Phys. Status Solidi* a **208** 52–8

[14] Sun D, Mazumder V, Metin O and Sun S 2011 Catalytic hydrolysis of ammonia borane via cobalt palladium nanoparticles *ACS Nano* **5** 6458–64

[15] Wang L Y *et al* 2005 Monodispersed core–shell Fe_3O_4@Au nanoparticles *J. Phys. Chem.* B **109** 21593–601

[16] Woo K *et al* 2004 Easy synthesis and magnetic properties of iron oxide nanoparticles *Chem. Mater.* **16** 2814–8

[17] Kotoulas A *et al* 2011 The role of synthetic parameters in the magnetic behavior of relative large hcp Ni nanoparticles *J. Nanopart. Res.* **13** 1897–908

[18] Naidek K P *et al* 2011 Structure and morphology of spinel MFe(2)O(4) (M = Fe, Co, Ni) nanoparticles chemically synthesized from heterometallic complexes *J. Colloid Interface Sci.* **358** 39–46

[19] Shavel A, Rodriguez-Gonzalez B, Pacifico J, Spasova M, Farle M and Liz-Marzan L M 2009 Shape control in iron oxide nanocrystal synthesis, induced by trioctylammonium ions *Chem. Mater.* **21** 1326–32

[20] Kim S-G, Terashi Y, Purwanto A and Okuyama K 2009 Synthesis and film deposition of Ni nanoparticles for base metal electrode applications *Colloids Surf.* A **337** 96–101

[21] Chen Z, Xu A, Zhang Y and Gu N 2010 Preparation of NiO and CoO nanoparticles using M 2+−oleate (M = Ni, Co) as precursor *Curr. Appl. Phys.* **10** 967–70

[22] Park J *et al* 2004 Ultra-large-scale syntheses of monodisperse nanocrystals *Nat. Mater.* **3** 891–5

[23] Kwon S G *et al* 2007 Kinetics of monodisperse iron oxide nanocrystal formation by 'heating-up' process *J. Am. Chem. Soc.* **129** 12571–84

[24] Xu Z, Shen C, Hou Y, Gao H and Sun S 2009 Oleylamine as both reducing agent and stabilizer in a facile synthesis of magnetite nanoparticles *Chem. Mater.* **21** 1778–80

[25] Zhang Y, Liu D, Wang X, Song S and Zhang H 2011 Synthesis of ferrite nanocrystals stabilized by ionic-liquid molecules through a thermal decomposition route *Chem. Eur. J.* **17** 920–4

[26] Oliveira F C C *et al* 2011 Ionic liquids as recycling solvents for the synthesis of magnetic nanoparticles *Phys. Chem. Chem. Phys.* **13** 13558–64

[27] Mott D, Galkowski J, Wang L, Luo J and Zhong C-J 2007 Synthesis of size-controlled and shaped copper nanoparticles *Langmuir* **23** 5740–5

[28] Sun S H and Zeng H 2002 Size-controlled synthesis of magnetite nanoparticles *J. Am. Chem. Soc.* **124** 8204–5

[29] Liu X *et al* 2007 A study on gold nanoparticle synthesis using oleylamine as both reducing agent and protecting ligand *J. Nanosci. Nanotechnol.* **7** 3126–33

[30] Crouse C A and Barron A R 2008 Reagent control over the size, uniformity, and composition of Co–Fe–O nanoparticles *J. Mater. Chem.* **18** 4146–53

[31] Klokkenburg M, Hilhorst J and Erne B H 2007 Surface analysis of magnetite nanoparticles in cyclohexane solutions of oleic acid and oleylamine *Vib. Spectrosc.* **43** 243–8

[32] Bronstein L M *et al* 2007 Influence of iron oleate complex structure on iron oxide nanoparticle formation *Chem. Mater.* **19** 3624–32

[33] Kim D, Lee N, Park M, Kim B H, An K and Hyeon T 2008 Synthesis of uniform ferrimagnetic magnetite nanocubes *J. Am. Chem. Soc.* **131** 454–5

[34] Roca A G, Morales M P and Serna C J 2006 Synthesis of monodispersed magnetite particles from different organometallic precursors *IEEE Trans. Magn.* **42** 3025–9

[35] Barbeta V B, Jardim R F, Kiyohara P K, Effenberger F B and Rossi L M 2010 Magnetic properties of Fe_3O_4 nanoparticles coated with oleic and dodecanoic acids *J. Appl. Phys.* **107** 073913

[36] Berti I O P D *et al* 2013 Alternative low-cost approach to the synthesis of magnetic iron oxide nanoparticles by thermal decomposition of organic precursors *Nanotechnology* **24** 175601

[37] Harris R A, Shumbula P M and van der Walt H 2015 Analysis of the interaction of the surfactants oleic acid and oleylamine with iron oxide nanoparticles through molecular mechanics modelling *Langmuir* **31** 3934–43

[38] Vargas J M, Nunes W C, Socolovsky L M, Knobel M and Zanchet D 2005 Effect of dipolar interaction observed in iron-based nanoparticles *Phys. Rev.* B **72** 184428

[39] Masunaga S H, Jardim R F and Rivas J 2011 Effect of weak dipolar interaction on the magnetic properties of Ni nanoparticles assembly analyzed with different protocols *J. Appl. Phys.* **109** 07B521

[40] Tronc E *et al* 1995 Magnetic dynamics of gamma-Fe_2O_3 nanoparticles *Nanostruct. Mater.* **6** 945–8